Successful Versus Failed Adaptation to High-Fat Diet–Induced Insulin Resistance

The Role of IAPP-Induced β-Cell Endoplasmic Reticulum Stress

Aleksey V. Matveyenko, Tatyana Gurlo, Marie Daval, Alexandra E. Butler, and Peter C. Butler

OBJECTIVE—Obesity is a known risk factor for type 2 diabetes. However, most obese individuals do not develop diabetes because they adapt to insulin resistance by increasing β-cell mass and insulin secretion. Islet pathology in type 2 diabetes is characterized by β-cell loss, islet amyloid derived from islet amyloid polypeptide (IAPP), and increased β-cell apoptosis characterized by endoplasmic reticulum (ER) stress. We hypothesized that IAPP-induced ER stress distinguishes successful versus unsuccessful islet adaptation to insulin resistance.

RESEARCH DESIGN AND METHODS—To address this, we fed wild-type (WT) and human IAPP transgenic (HIP) rats either 10 weeks of regular chow or a high-fat diet and prospectively examined the relations among β-cell mass and turnover, β-cell ER stress, insulin secretion, and insulin sensitivity.

RESULTS—A high-fat diet led to comparable insulin resistance in WT and HIP rats. WT rats compensated with increased insulin secretion and β-cell mass. In HIP rats, in contrast, neither β-cell function nor mass compensated for the increased insulin demand, leading to diabetes. The failure to increase β-cell mass in HIP rats was the result of ER stress–induced β-cell apoptosis that increased in proportion to diet-induced insulin resistance.

CONCLUSIONS—IAPP-induced ER stress distinguishes the successful versus unsuccessful islet adaptation to a high-fat diet in rats. These studies are consistent with the hypothesis that IAPP oligomers contribute to increased β-cell apoptosis and β-cell failure in humans with type 2 diabetes. ***Diabetes* 58: 906–916, 2009**

Insulin resistance, most often attributed to high-caloric food intake and consequent obesity (1), is a well-characterized risk factor for type 2 diabetes (2,3). However, most obese individuals (>80%) do not develop diabetes (4) because they are able to compensate for insulin resistance by an adaptive increase in insulin secretion (5,6). Type 2 diabetes develops as a result of a failure to adequately increase insulin secretion to meet demands of insulin resistance (5,7,8). Consistent with this, genomewide studies imply that the genetic variance that underlies predisposition to type 2 diabetes is manifest in pancreatic β-cells (9–11). By implication, there is a subset of individuals in the general population at risk of developing type 2 diabetes if subject to insulin resistance. These observations raise the question, what underlies the failure of β-cell adaptation to insulin resistance in those predisposed to type 2 diabetes?

Some insights arise from the pathology of the islet in type 2 diabetes. There is a 60% deficit in β-cells in individuals who are obese with type 2 diabetes compared with those comparably obese but nondiabetic (12,13). The islet in type 2 diabetes is also characterized by islet amyloid derived from islet amyloid polypeptide (IAPP) (12). High expression rates of human IAPP in some rodent models recapitulate this islet pathology and lead to diabetes (14–17). In the HIP rat (Sprague-Dawley rats transgenic for human IAPP), there is a gradual decline in β-cell mass leading to impaired fasting glucose at 5 months of age and diabetes by 10 months of age (16,18). In both humans with type 2 diabetes (12) and rodents with high expression rates of human IAPP, there is increased β-cell apoptosis characterized by endoplasmic reticulum (ER) stress (19,20). β-Cell loss, therefore, in type 2 diabetes has many parallels with that in neurodegenerative diseases also characterized by protein misfolding (21). In Alzheimer's and Parkinson's disease, for example, neuronal cell loss is characterized by increased ER stress–induced apoptosis accompanied by formation of toxic oligomers of locally expressed amyloidogenic proteins (22). Collectively these diseases have been referred to as protein misfolding diseases.

In occasional families, protein misfolding diseases can be attributed to a mutation that increases the propensity of the respective amyloidogenic protein to aggregate (23). In most cases, however, the basis for protein misfolding is not the result of a mutant amyloidogenic protein, but rather a consequence of an imbalance between the delivery of nascent protein to the ER and the capacity of the ER to fold, traffic, and process the protein (22). Support for the concept of a threshold of expression rate above which ER fails to adequately process IAPP is provided by human IAPP transgenic rodent models recently reviewed elsewhere (24). Given the complexity of ER function (including calcium homeostasis, chaperone proteins, glycosylation, clearance of misfolded proteins), it is likely that this threshold varies widely between individuals within the population, perhaps contributing to the genetic variance in predisposition to type 2 diabetes. It is of

From the Larry Hillblom Islet Research Center, David Geffen School of Medicine at the University of California, Los Angeles, Los Angeles, California.

Corresponding author: Aleksey V. Matveyenko, amatveyenko@mednet.ucla.edu.

Received 23 October 2008 and accepted 6 January 2009.

Published ahead of print at http://diabetes.diabetesjournals.org on 16 January 2009. DOI: 10.2337/db08-1464.

note that IAPP expression increases with insulin resistance (25).

It is therefore plausible that the link between the increased risk for type 2 diabetes in obesity is mediated through an imbalance between the delivery of nascent IAPP to the ER and the capacity of the ER to fold, traffic, and process this amyloidogenic protein in vulnerable individuals. It is not possible to address this hypothesis experimentally in humans. To gain insight into this postulate, we undertook studies in wild-type (WT) Sprague-Dawley rats and Sprague-Dawley rats transgenic for human IAPP (HIP rats) on a high-fat diet (HFD). We hypothesized that WT rats would adapt to an HFD to remain nondiabetic, whereas HIP rats would fail to adapt and would develop diabetes. This hypothesis was affirmed, permitting us to further establish the molecular, pathological, and physiological basis of successful versus failed adaptation to an HFD in vivo as well as at the level of the pancreas.

RESEARCH DESIGN AND METHODS

Animal housing, diet administration, and surgical procedures. A total of 54 Sprague-Dawley rats (WT; $n = 25$) and rats expressing human IAPP (HIP rats; $n = 29$) were used. The generation of the human IAPP transgenic rats has been described in detail previously (16). Rats were bred and housed individually throughout the study at the University of California, Los Angeles (UCLA) animal housing facility and subjected to a standard 12-h light-dark cycle. The UCLA Institutional Animal Care and Use Committee approved all surgical and experimental procedures. At 2 months of age, WT and HIP rats were randomly assigned to either an HFD (60% fat, 20% protein, and 20% carbohydrates; Research Diets, New Brunswick, NJ) or a control regular chow diet (10% fat, 20% protein, and 70% carbohydrates; Research Diets) and fed ad libitum for 10 weeks. After 10 weeks of either diet, treatment animals were anesthetized with isoflurane (2.5%) by inhalation until effect, and indwelling catheters were then inserted into the right internal jugular vein and left carotid artery for subsequent in vivo metabolic studies as previously described (26). All catheters were filled with 100 U/ml heparin/saline solution, exteriorized to the back of the neck, and encased in the infusion harness (Instech, Plymouth Meeting, PA). After surgery, all rats maintained preoperative body weight and had normal food intake and mean hematocrit (>40%).

Hyperglycemic clamp and arginine bolus injection. To assess glucose and arginine-stimulated insulin secretion, HIP ($n = 10$), HIP + HFD ($n = 9$), WT ($n = 6$), and WT + HFD ($n = 12$) rats underwent a hyperglycemic clamp followed by an arginine bolus injection as previously described (18). In brief, after a 30-min equilibration period, plasma samples were taken for measurements of fasting glucose, insulin, C-peptide, and free fatty acids. Thereafter, animals received an intravenous glucose bolus (375 mg/kg) followed by a variable 50% (wt/vol) glucose infusion to clamp arterial glucose at ~250 mg/dl (0–70 min). At 60 min, rats received a bolus injection of L-arginine solution (1 mmol/kg; Sigma, St. Louis, MO). Arterial blood samples (50 μl) were taken at baseline (−30 and 0 min), at 1 and 5 min, and every 15 min thereafter during the clamp for immediate determination of plasma glucose and subsequent analysis for insulin and C-peptide.

Hyperinsulinemic-euglycemic clamp + ^{3}H-glucose infusion. To assess insulin sensitivity and glucose turnover, HIP ($n = 7$), HIP + HFD ($n = 7$), WT ($n = 6$), and WT + HFD ($n = 7$) rats underwent a hyperinsulinemic-euglycemic clamp with concomitant infusion of [3-^{3}H]glucose to assess glucose turnover as previously described (18). Rats received primed (3 μCi) continuous (0.05 μCi/min) infusion of [3-^{3}H]glucose (Perkin Elmer, Boston, MA) for a 90-min basal period increased to 0.2 μCi/min for 120 min throughout the hyperinsulinemic-euglycemic clamp. Plasma glucose was determined every 10 min, and additional blood samples (~150 μl) for determination of tracer-specific activity at fasting were drawn from −40 to 0 min and during insulin infusion from 120 to 150 min.

Pancreas morphology. At the end of the hyperinsulinemic-euglycemic clamp, rats were euthanized and the pancreas was then rapidly removed and fixed in 4% paraformaldehyde overnight at 4°C. Paraffin-embedded pancreatic sections were stained first for hematoxylin and eosin, insulin (guinea pig anti-insulin, 1:100; Zymed, Carlsbad, CA). The β-cell mass was measured by quantifying the pancreatic cross-sectional area positive for insulin and multiplying this by the pancreatic weight. β-Cell size was determined as a mean distance between neighboring insulin-positive nuclei in 10 representative islets per animal. β-Cell nuclear diameter was determined as a mean (of 180 measurements per nucleus) nuclear diameter in insulin-positive nuclei in 10 representative islets per animal. Sections were also costained by immunofluorescence for insulin (guinea pig anti-insulin, 1:100; Zymed) and terminal deoxynucleotidyl transferase biotin-dUTP nick-end labeling (TUNEL method; Roche Diagnostics, Mannheim, Germany) for quantification of β-cell apoptosis and insulin (guinea pig anti-insulin, 1:100; Zymed) and Ki-67 (mouse anti–Ki-67, 1:50; Dako, Carpinteria, CA) for determination of β-cell replication. Additional sections were costained by immunofluorescence for insulin (guinea pig anti-insulin, 1:100; Zymed) and anti-C/EBP homologous protein (CHOP) (rabbit ant-CHOP; Santa Cruz Biotechnology) as previously described in detail (19,20). All islets per pancreatic section (~100 islets) were examined in detail at ×200 magnification (×20 objective, ×10 ocular) for the total number of TUNEL, Ki-67, and CHOP-positive β-cells. The frequency of TUNEL, Ki-67, and CHOP expression in each animal was presented as total number of stained β-cells per total number of islets. Fluorescent slides were analyzed and imaged using a Leica DM600 microscope (Leica Microsystems, Wetzlar, Germany), and images were acquired using OpenLab software (Improvision) and analyzed using ImagePro Plus software.

Islet isolation and Western blotting. To obtain rat islets, HIP ($n = 4$), HIP + HFD ($n = 4$), WT ($n = 3$), and WT + HFD ($n = 3$) rats were euthanized, and islets were isolated as previously described (19). For Western blotting experiments, islets were washed with ice-cold PBS and lysed in 2× Laemmli sample buffer immediately following the isolation procedure. Proteins (50 μg/lane) were separated on a 4% to 12% Bis-Tris NuPAGE gel and transferred to polyvinylidine fluoride membranes (Bio-Rad). Membranes were blocked with 5% nonfat dry milk in TBS/0.1% Tween-20 and incubated overnight at 4°C with CHOP (1:500; Santa Cruz Biotechnology), anti-P-PERK (1:2,000; Cell Signaling Technology, Beverly, MA), anti-GRP78 (1:10,000; Stressgen, Victoria, BC, Canada), anti-hIAPP (1:6,000, 25–37 aa; Peninsula Laboratories, San Carlos, CA), anti-insulin (1:100; Zymed), and anti-GAPDH (1:8,000; Cell Signaling Technologies). Membranes were washed with TBS/0.1% Tween-20 and incubated with horseradish peroxidase–conjugated secondary antibodies (1:3,000; Jackson Laboratories, Bar Harbor, ME) for 1 h. After washes, proteins were visualized using enhanced chemiluminescence (Bio-Rad) and protein expression levels were quantified using UN-SCAN-IT software (Silk Scientific, Orem, UT).

Analytical procedures. Plasma glucose concentrations were measured by the glucose oxidase method (Beckman Glucose Analyzer 2; Beckman, Fullerton, CA). Plasma insulin and C-peptide levels were measured using ELISA assay (Alpco Diagnostics, Salem, NH). Plasma free fatty acid levels were measured using in vitro standard enzymatic colorimetric methods (WAKO Chemicals, Richmond, VA). Plasma glucose specific activity, hepatic glucose production, and glucose disposal were calculated as previously described in detail (18).

Statistical analysis was performed using ANOVA analysis with Fisher's post hoc where appropriate. Regression analysis was performed using Statistica, Version 6 (Statsoft, Tulsa, OK). Data in graphs and tables are presented as means ± SEM. Findings were assumed statistically significant at $P < 0.05$.

RESULTS

Development of diet-induced diabetes in HIP rats on an HFD. Food intake, body weight, and plasma free fatty acid levels increased comparably in WT and HIP rats on an HFD (Fig. 1*B* and *C*; Table 1). The fasting plasma glucose concentrations in HIP and WT rats were comparable at the beginning of the study ($P = 0.85$ between groups). On a regular chow diet, fasting plasma glucose values remained unchanged in the WT rats but increased to the impaired fasting glucose concentration range in the HIP rats, consistent with prior studies over the same age range (16,18). On the HFD, there was a modest increase in blood glucose in WT rats (110 ± 3 versus 98 ± 2 mg/dl; P = nonsignificant for WT + HFD versus WT; Fig. 1*A*), but in contrast, HIP + HFD rats developed diabetes (178 ± 20 mg/dl; $P < 0.0001$ versus all other groups; Fig. 1*A*). Although there was no relation between change in either body weight or food intake and the fasting blood glucose concentration in WT rats, both food intake ($r = 0.9$, $P < 0.01$) and increase in body weight ($r = 0.9$, $P < 0.01$) during the 10-week study predicted the subsequent fasting blood glucose concentrations in HIP rats (Fig. 1*D* and *E*).

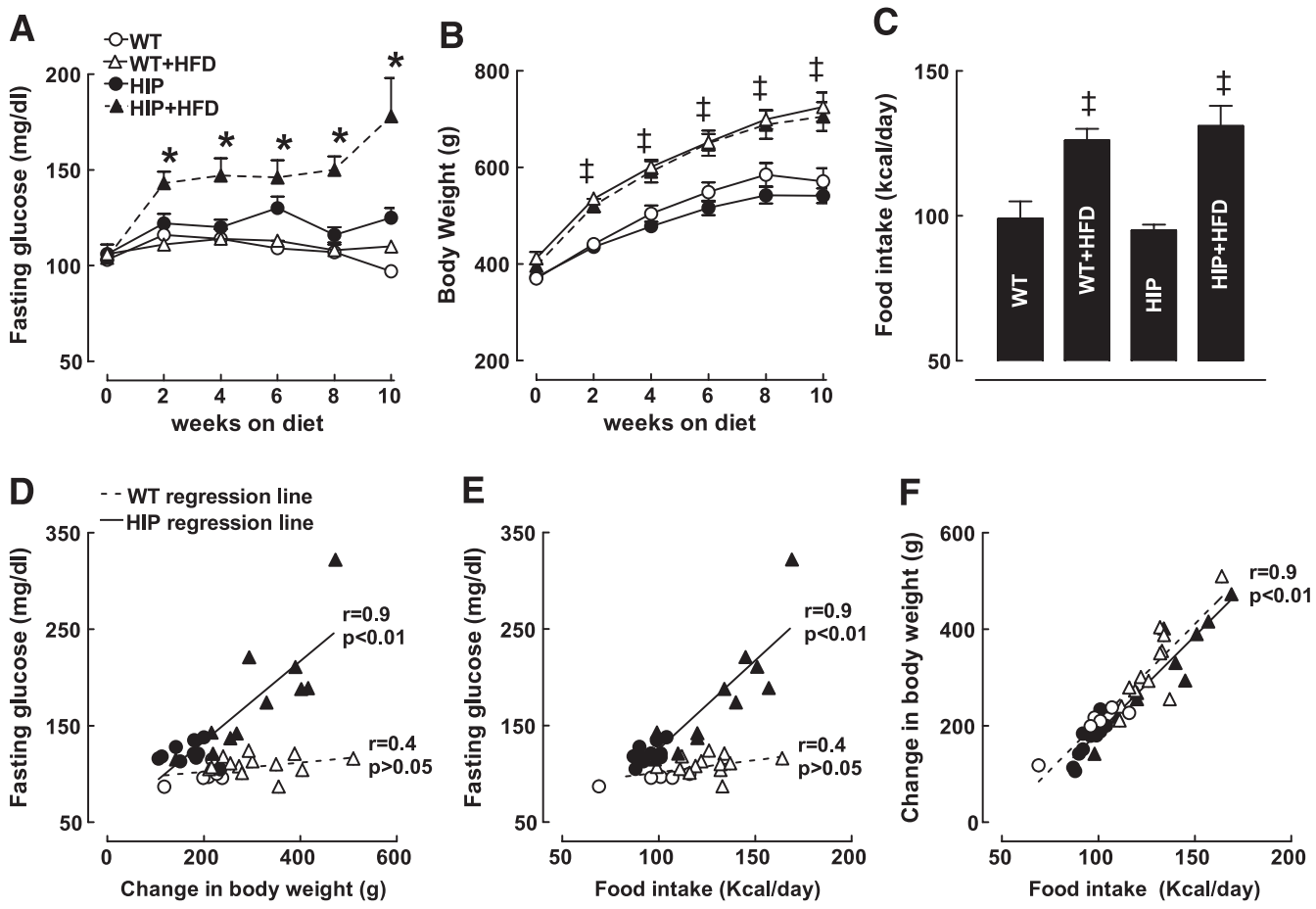

FIG. 1. Development of diet-induced diabetes in HIP rats on an HFD. Fasting plasma glucose (*A*), body weight (*B*), and mean daily food intake (*C*) during 10-week treatment with 60% high fat (HFD) or regular chow diet in WT (n = 19) and HIP rats (n = 21). The relationship between the change in body weight (*D*) and daily caloric food intake (*E*) versus fasting glucose levels in HIP rats (*solid line*) and WT rats (*broken line*) during 10-week treatment with 60% HFD or regular chow diet. *F*: The relation between the mean daily caloric food intake and change in body weight in individual WT rats (*broken line*) and HIP rats (*solid line*). Data are means ± SE. *P < 0.001 for HIP + HFD versus all groups; ‡P < 0.001 for regular chow versus HFD. ○, WT; △, WT + HFD; ●, HIP; ▲, HIP + HFD.

Failure of the compensatory increase in β-cell mass in HIP rats. The HFD provoked a 46% increase in β-cell mass in WT rats (13 ± 2 versus 19 ± 2 mg, WT versus WT + HFD; $P < 0.05$), but no change of β-cell mass in HIP rats (12 ± 1 versus 13 ± 2 mg, HIP versus HIP+HFD; P = nonsignificant; Fig. 2*A* and *B*). The increase in β-cell mass in WT rats on an HFD was the result of β-cell hyperplasia rather than hypertrophy because β-cell size and nuclear diameter were unchanged (Fig. 2*D* and *E*). β-Cell apoptosis was increased almost 13-fold (0.04 ± 0.006 versus 0.003 ± 0.001 cells/islet; Fig. 3*A* and *C*, $P <$ 0.001) in HIP versus WT rats on a regular diet, but this was partially offset by a sixfold increase in β-cell replication (0.018 ± 0.003 versus 0.003 ± 0.003 cells/islet; Fig. 3*B* and *D*). Although there was no increase (P = 0.22) in β-cell apoptosis in WT rats on an HFD, β-cell apoptosis increased still further in HIP rats on the HFD (Fig. 3*A* and *C*, $P < 0.0001$, 34-fold versus WT rats). In contrast, there was no further increase in β-cell replication in HIP rats on the HFD (Fig. 3*B* and *D*).

Unfolded protein response and ER stress and high-fat feeding in WT versus HIP rats. To further elucidate the underlying mechanism by which an HFD led to increased β-cell apoptosis in the HIP rats but not the WT rats, we next investigated the unfolded protein response (P-PERK and GRP-78) and ER stress by examining the protein expression

TABLE 1
Metabolic characteristics of HIP and WT rats after 10 weeks on an HFD or regular chow diet

	WT	WT + HFD	HIP	HIP + HFD
n	6	13	10	11
Weight (g)	571 ± 27	725 ± 30*	541 ± 15	705 ± 30*
Fasting glucose (mg/dl)	98 ± 2	110 ± 3	121 ± 3	178 ± 20†
Fasting insulin (pmol/l)	299 ± 57	610 ± 80*	179 ± 28	518 ± 113*
Fasting C-peptide (ng/ml)	1.9 ± 0.2	3.1 ± 0.5*‡	1.3 ± 0.2	1.8 ± 0.2
Fasting free fatty acids (mmol/l)	0.4 ± 0.1	1.1 ± 0.4	0.5 ± 0.1	0.8 ± 0.2

Data are expressed as means ± SEM. *$P < 0.05$ for HFD versus regular chow. †$P < 0.05$ for HIP + HFD versus all other groups. ‡$P < 0.05$ for WT + HFD versus all groups.

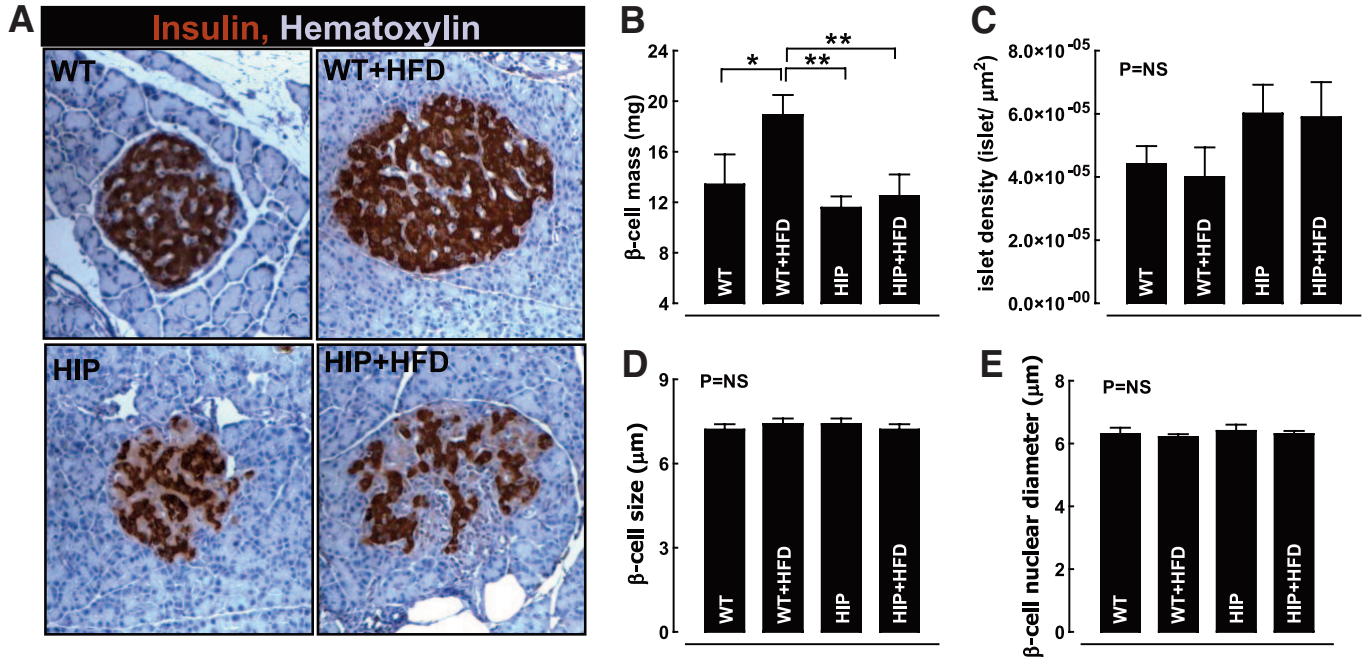

FIG. 2. Compensatory increase in β-cell mass in response to an HFD is absent in HIP rats. *A*: Typical islets from wild-type (WT) and HIP rats stained for insulin and hematoxylin after 10 weeks of 60% high-fat (HFD) or regular chow diet. Quantification of β-cell mass (*B*), mean islet number per section (*C*), mean β-cell size (*D*), and β-cell nuclear diameter (*E*) after 10 weeks of 60% HFD or regular chow diet in WT (n = 19) and HIP rats (n = 21). Data are means ± SE. *P < 0.05; **P < 0.01. (A high-quality digital representation of this figure is available in the online issue.)

and nuclear colocalization of the ER stress marker CHOP. In WT rats, the HFD increased both PERK phosphorylation and GRP78 expression in relation to the primary ER client protein insulin (Fig. 4*A*–*C*). In HIP rats, P-PERK and GRP78 expression were already increased on a regular chow diet in comparison to WT rats in relation to insulin expression. In HIP rats, however, neither P-PERK nor GRP78 expression were further increased in response to the HFD (Fig. 4*B* and *D*) despite the further increased expression of both insulin and IAPP, so the protective unfolded protein response was not further increased in the HFD-fed rats despite this marked increased ER load. Nuclear CHOP expression was 13-fold increased in HIP versus WT rats on a regular diet (0.049 ± 0.011 versus 0.0037 ± 0.002 β-cells/islet, P < 0.01; Fig. 4*D*–*E*) and was increased further in HIP, but not WT, rats with an HFD (0.049 ± 0.011 versus 0.09 ± 0.01 β-cells/islet, P < 0.01; Fig. 4*D* and *E*). There was a positive correlation between the frequency of β-cell nuclear CHOP and β-cell apoptosis (r = 0.6, P < 0.001; Fig. 4*F*). Western blot analysis of protein lysates from isolated islets confirmed the immunohistochemically detected increased CHOP protein expression in HIP rats on a regular diet increased further on the HFD (Fig. 4*A*). These data reveal that an HFD exacerbated ER stress–induced apoptosis in the HIP rat, but did not induce ER stress in WT rats, implying that the propensity of human IAPP to form toxic oligomers is an important link between an HFD and ER stress–induced β-cell apoptosis.

HIP rats fail to adaptively increase fasting, glucose-stimulated, and arginine-stimulated insulin secretion in response to HFD and have impaired hepatic insulin clearance. In the fasting state, insulin secretion was impaired in HIP rats on an HFD, as illustrated by failure to increase C-peptide concentrations despite hyperglycemia (Fig. 5*A*, *D*, and *G*). In contrast, C-peptide concentrations increased by 1.6-fold in WT rats on an HFD (1.9 ± 0.2 versus 3.1 ± 0.5 ng/ml, P < 0.05; Fig. 5*A*, *D*, and *G*) in response to an HFD. In contrast, although insulin secretion was impaired in HIP rats in the fasting state (evaluated by C-peptide concentrations), systemic insulin concentrations were comparable to those in WT rats (Table 1), indicating that hepatic insulin clearance of endogenously secreted insulin was decreased in HIP rats on a chow diet or HFD. To evaluate glucose-mediated insulin secretion under comparable conditions, we performed hyperglycemic clamp studies in which, by design, plasma glucose levels were maintained at 265 ± 10 mg/dl (supplemental Fig. 1, available in an online appendix at http://diabetes.diabetesjournals.org/cgi/content/full/db08-1464). In response to HFD, in WT rats, the first-phase insulin response to glucose was increased by 1.7-fold (966 ± 90 versus 1,677 ± 108 pmol/l, P < 0.01, WT versus WT + HFD; Fig. 5*B*, *E*, and *H*) and the second phase by twofold (705 ± 33 versus 1,462 ± 116 pmol/l, P < 0.01, WT versus WT+HFD; supplemental Fig. 1, available in the online appendix). In contrast, in HIP rats, there was a markedly blunted first- and second-phase response to hyperglycemia and no increment with an HFD (Fig. 5*B*, *E*, and *H*). Likewise, although there was a 1.5-fold increase in arginine-stimulated insulin release in WT rats in response to an HFD, there was no increase in arginine-induced insulin secretion at the same glucose concentration in the HIP rat on a regular diet or HFD (Fig. 5*C*, *F*, and *I*). Consistent with these findings, we observed a positive correlation between β-cell mass and fasting C-peptide (r = 0.5, P < 0.01; Fig. 5*D* and *G*), first-phase insulin response to glucose (r = 0.4, P < 0.01; Fig. 5*E* and *H*), and first-phase insulin response to arginine (r = 0.5, P < 0.01; Fig. 5*F* and *I*).

HIP rats on an HFD exhibit increased fasting and insulin-stimulated hepatic glucose production. To further elucidate the relation between hepatic and extrahepatic insulin sensitivity and β-cell failure in HIP rats exposed to an HFD, we undertook hyperinsulinemic-

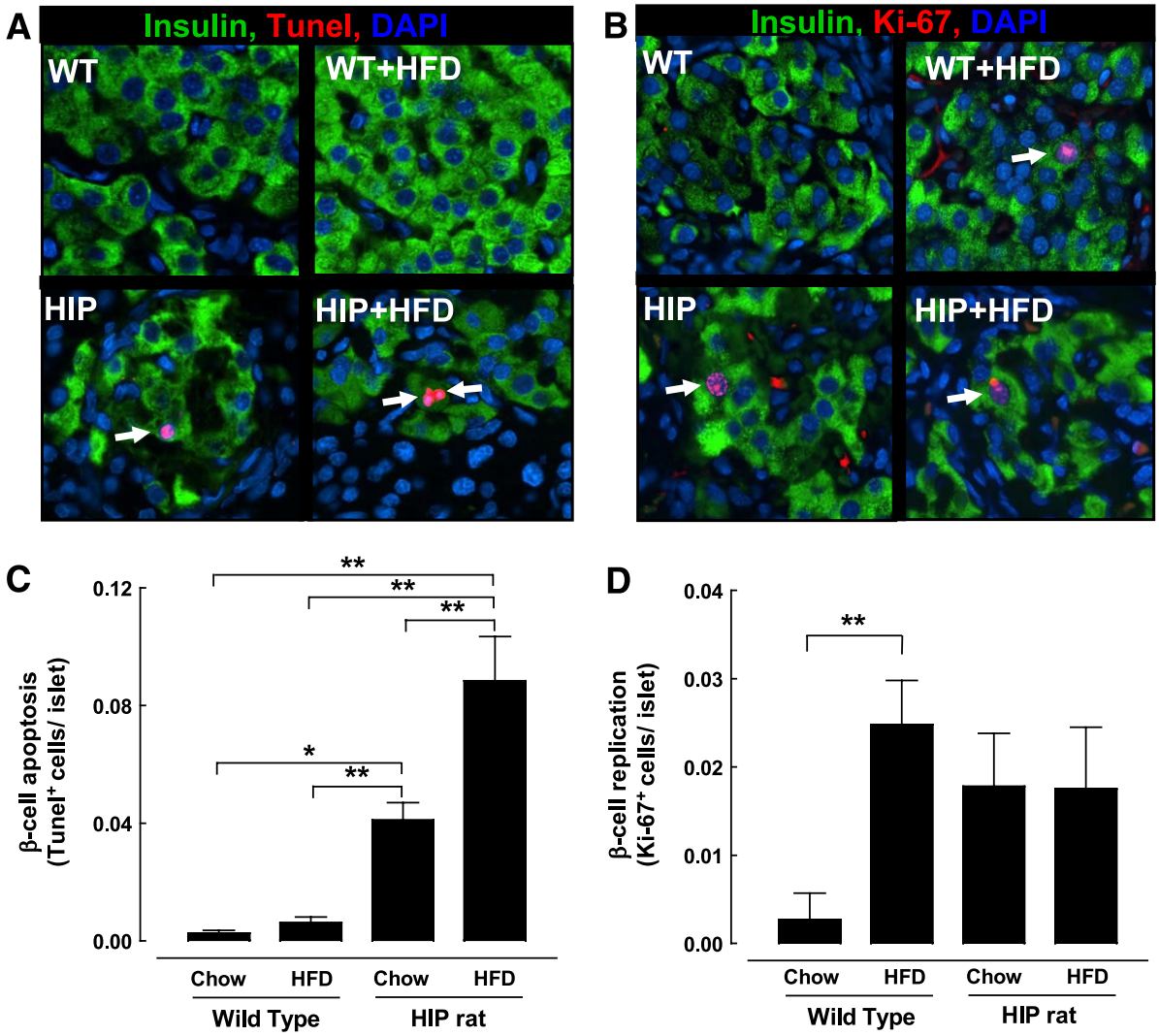

FIG. 3. HFD leads to increased β-cell apoptosis in HIP rats and increased β-cell replication in wild-type rats. *A* and *B*: Examples of islets stained for insulin (*green*) and apoptosis marker TUNEL (*red*) (*A*) and islets stained for insulin and replication marker Ki-67 (*red*) and nuclear stain DAPI (*blue*) (*B*) imaged at 200×. *C* and *D*: Quantified frequency of β-cell apoptosis and replication after 10 weeks of 60% HFD or regular chow diet in WT (n = 19) and HIP rats (n = 21). Data are means ± SE. *$P < 0.05$; **$P < 0.01$. Note that the frequency of TUNEL- and Ki67-positive cells in islets shown in *A* and *B* are higher than the mean to reveal the fidelity of the immunostaining rather than representative of the mean. (A high-quality digital representation of this figure is available in the online issue.)

euglycemic clamps while measuring glucose turnover. By design, plasma glucose and insulin concentrations were comparable during the hyperinsulinemic-euglycemic clamps in HIP and WT rats on a regular chow diet or HFD (Fig. 6*A*). Whole-body insulin sensitivity, assessed by the mean glucose infusion rates during the hyperinsulinemic clamp, was comparably decreased by HFD in HIP and WT rats (Fig. 6*B*). The isotope dilution technique revealed that fasting hyperglycemia in the HIP + HFD group was attributed to a twofold increase in fasting hepatic glucose production (Fig. 6*C*, $P < 0.05$ versus all other groups). In HIP rats, there was hepatic insulin resistance (impaired suppression of hepatic glucose release during the clamp) (Fig. 6*C*). Isotopically measured insulin-stimulated glucose uptake was comparably decreased by HFD in both HIP and WT rats (Fig. 6*D*). An HFD had its primary effect on insulin sensitivity by inducing extrahepatic insulin resistance, whereas the HIP rat has a selective defect in hepatic insulin sensitivity independent of the HFD.

The interaction between insulin sensitivity and successful versus failed β-cell adaptation. In summary, WT and HIP rats provided either a regular chow diet or HFD for 10 weeks had an average daily food intake that varied from 100 to 200 Kcal/day. Weight gain and subsequent insulin resistance was proportionate to average food intake, which was comparable in WT and HIP rats. In WT rats, β-cell mass and function successfully adapted to insulin resistance. The adaptive increase in β-cell mass was accomplished by increased β-cell replication in the absence of any increase in β-cell apoptosis (Fig. 7*B*, *D*, and *F*). In contrast, in HIP rats, neither β-cell function nor mass adaptively increased to the increased demand imposed by an HFD (Fig. 7*E*). In HIP rats, increasing insulin resistance provoked increased β-cell apoptosis (Fig. 7*A*) but with no effective increase in β-cell replication (Fig. 7*B*).

DISCUSSION

An HFD leads to obesity and insulin resistance (1) that in most individuals is compensated by increased β-cell mass

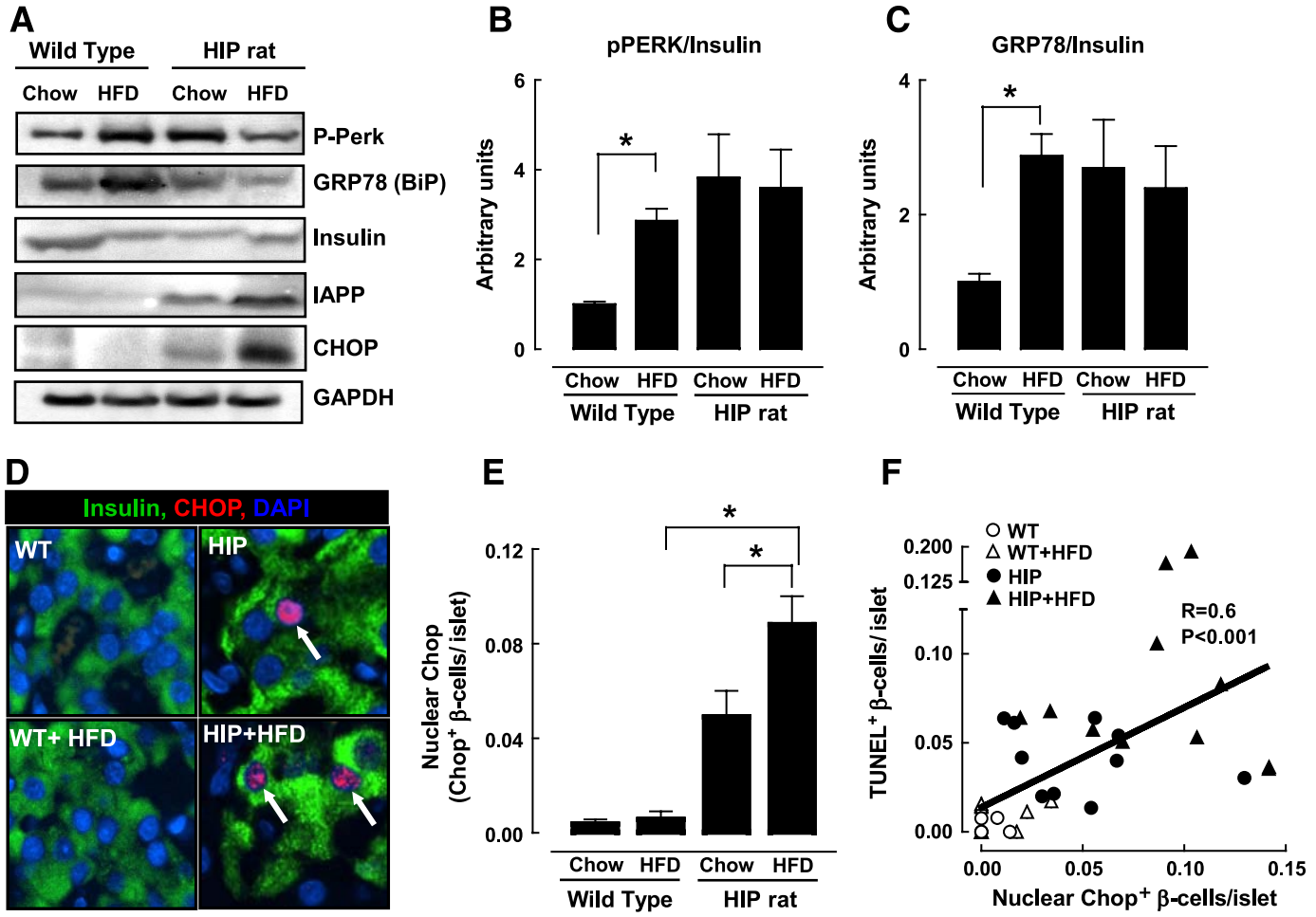

FIG. 4. HFD leads to increased ER stress in HIP rats. ***A*****: Immunoblot analysis of P-PERK, GRP-78, insulin, IAPP, and CHOP in protein lysates from islets isolated after 10 weeks of a 60% HFD or regular chow diet in WT (n = 6) and HIP rats (n = 8).** ***B*** **and** ***C*****: Quantification of P-PERK and GRP-78 expression normalized to insulin expression.** ***D*****: Representative examples of islets stained by immunofluorescence for insulin (*green*), ER stress marker CHOP (*red*), and nuclear stain DAPI (*blue*) imaged at 200×.** ***E*** **and** ***F*****: Quantified frequency of nuclear CHOP expression per islet and (*E*) a relation between the frequency of β-cell CHOP versus TUNEL expression after 10 weeks of 60% HFD or regular chow diet (*F*) in WT (n = 19) and HIP rats (n = 21) rats. Data are means ± SE. *P < 0.05; **P < 0.05. Note that the frequency of CHOP-positive cells in islets shown in *D* are higher than the mean to reveal the fidelity of the immunostaining rather than representative of the mean. (A high-quality digital representation of this figure is available in the online issue.)**

and insulin secretion (6,12). In those vulnerable to type 2 diabetes, hyperglycemia occurs as a consequence of impaired insulin secretion in response to insulin resistance (27,28) with characteristic islet pathology including a deficit in β-cell mass (12,13), islet amyloid derived from IAPP, and ER stress–induced β-cell apoptosis (20,29). We sought to gain insights into the mechanisms underlying the appropriate adaptive versus maladaptive β-cell response to HFD-induced insulin resistance.

In humans, prospective measurements of the adaptive changes in β-cell mass and corresponding changes in insulin secretion and insulin resistance in response to obesity are unavailable because longitudinal studies of pancreatic morphology cannot be performed. Cross-sectional studies of islet morphology in humans report a 50% increase in β-cell mass in obese individuals compared with their lean counterparts (12). Similarly, cross-sectional studies that examined changes in insulin secretion and insulin sensitivity in obesity report an ~1.5- to 3-fold increase in fasting and meal-stimulated insulin secretion (6,7,28) and an ~50% decrease in insulin sensitivity (28,30). We report that 10 weeks of high-fat feeding initiated at 2 months of age in the Sprague-Dawley rat induced a 46% increase in β-cell mass and a 1.5- to 2-fold increase in fasting and glucose-stimulated insulin secretion in response to a 50% decline in whole body insulin sensitivity. The adaptive changes in the WT rat on an HFD therefore recapitulate those observed in nondiabetic obese humans. We report for the first time in the same animals that the adaptive changes in insulin secretion in WT + HFD animals is closely related to the adaptive increase in β-cell mass.

In contrast to WT rats, HIP rats failed to adaptively increase β-cell mass and insulin secretion in response to HFD-induced insulin resistance. β-Cell replication was increased in HIP rats compared with WT rats at baseline, but this increased β-cell replication was offset by increased β-cell apoptosis so that β-cell mass was comparable in WT and HIP rats. β-Cell replication failed to increase further in HIP rats on an HFD despite a marked further increase in β-cell apoptosis, consistent with prior studies showing that newly forming β-cells have increased vulnerability to IAPP-induced apoptosis (31). A primary goal of the present studies was to gain insights into the successful versus failed adaptation to high fat–induced obesity. Having noted that failure to expand

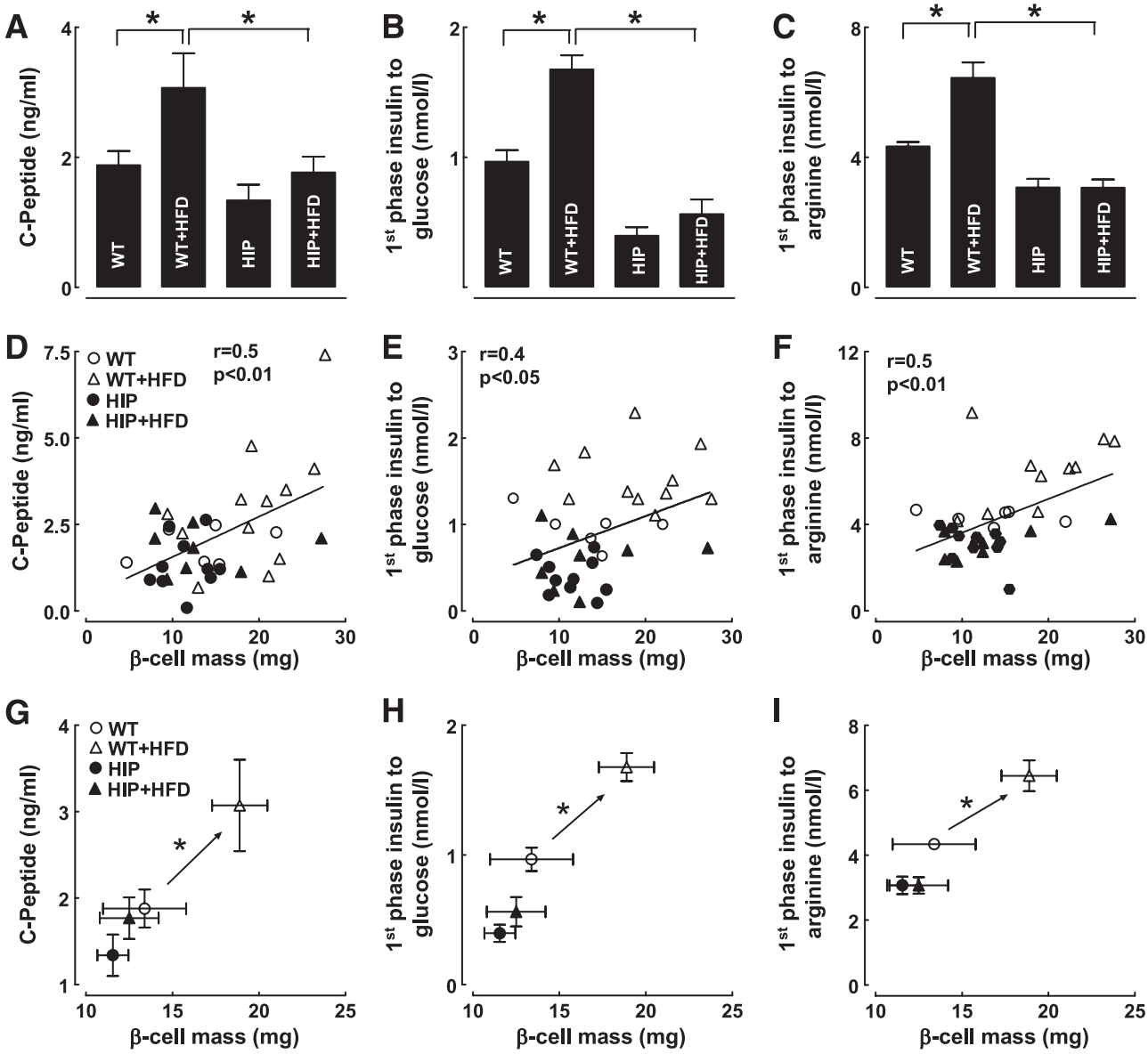

FIG. 5. HIP rats fail to adaptively increase fasting, glucose-stimulated, and arginine-stimulated insulin secretion in response to an HFD. Mean fasting C-peptide levels (*A*), first-phase glucose (*B*), and arginine-stimulated insulin secretion (*C*). *D–I*: Regression analysis of relations between changes in β-cell mass and fasting, glucose-stimulated, and arginine-stimulated insulin secretion in WT (n = 18) and HIP rats (n = 19) after 10-week treatment with 60% HFD or regular chow diet. Data are means ± SE. *P < 0.05; **P < 0.01.

β-cell mass in HIP rats fed an HFD was the result of ER stress–induced β-cell apoptosis, we turned our attention to the role of the ER in the successful versus failed adaptation to an HFD.

The ER in the β-cell is well developed to permit synthesis, folding, processing, and export of the primary client secretory proteins, insulin, and IAPP. The unfolded protein response (UPR) is an important adaptive regulatory mechanism that seeks to balance the rate of delivery of nascent proteins into the ER with the capacity of the ER to fold and export these proteins (32). The UPR accomplishes this both by constraining the rate of protein synthesis as well as enhancing the capacity of this system, for example, by increasing the ER chaperone protein BIP that binds to all nascent ER proteins as they are inserted into the ER (33). Evidence that the UPR was intact in WT rats is provided by increased PERK phosphorylation and GRP78 expression in relation to the primary ER client proteins insulin and IAPP. In contrast, although PERK phosphorylation and GRP78 expression were increased in HIP rats on a regular chow diet in comparison to WT rats, in relation to insulin expression, the UPR was not further increased in response to the HFD. It is therefore plausible that high expression rates of oligomeric proteins (such as human IAPP) may lead to ER stress, in part attributable to the failure of an adequate unfolded protein response. Consistent with action of CHOP to mediate ER stress–induced apoptosis, we observed a similar twofold increase in β-cell apoptosis in response to an HFD in HIP, but not in WT, rats. There was a positive correlation between nuclear CHOP and β-cell apoptosis (r = 0.6, P = 0.0001; Fig. 4*F*).

To underscore the postulate that β-cell ER stress–induced apoptosis is related to the extent of insulin resistance in those genetically vulnerable, the frequency of β-cell apoptosis was positively related to the degree of insulin resistance in HIP rats (P < 0.05), but not WT rats (P = 0.6). The close parallels in the islet pathology

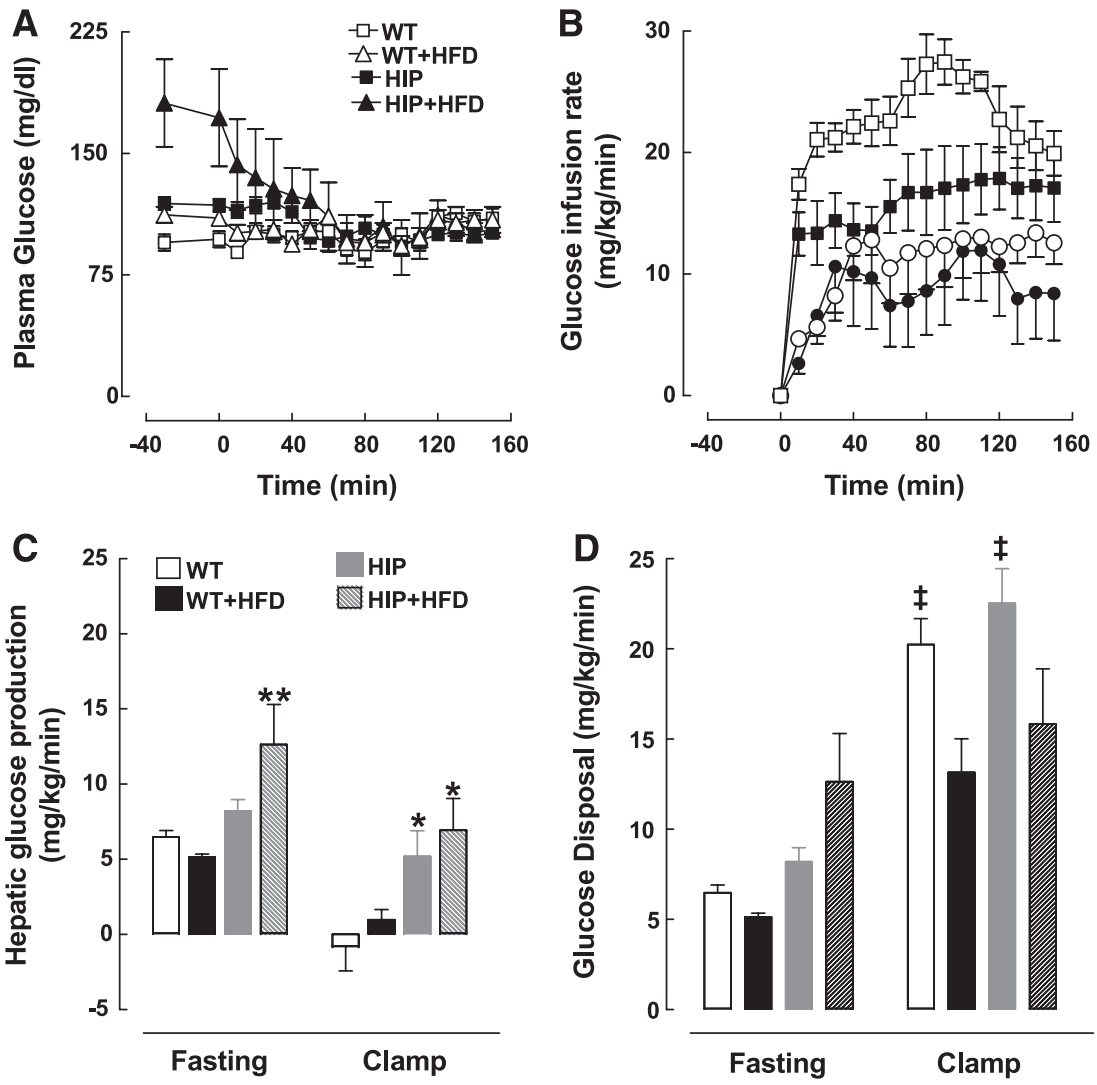

FIG. 6. HIP rats on HFD exhibit increased fasting and insulin-stimulated hepatic glucose production. *A*: Fasting (−30 and 0 min) and hyperinsulinemic-euglycemic clamp glucose concentrations. *B*: Mean glucose infusion rates required to maintain euglycemia during the hyperinsulinemic clamp. *C* and *D*: Mean rates of hepatic glucose production (*C*) and glucose disposal (*D*) at fasting and during the final 30 min of the hyperinsulinemic-euglycemic clamp in WT (n = 13) and HIP rats (n = 14) after 10-week treatment with 60% HFD or regular chow. Data are means ± SE. *P < 0.05 for HIP versus WT; **P < 0.05 for HIP + HFD versus all groups; ‡P < 0.05 for HFD versus chow.

between the HFD-fed HIP rat and obese humans with type 2 diabetes (β-cell deficit resulting from ER stress–induced β-cell apoptosis) are consistent with the postulate that humans genetically at risk of type 2 diabetes, like the HIP rat, have a marginal capacity for ER to traffic IAPP that is readily overcome by induction of insulin resistance. In contrast, humans who are not genetically vulnerable to type 2 diabetes are capable of adapting to insulin resistance and so presumably have a much higher threshold for expression and trafficking of IAPP.

We note that both WT and HIP rats developed comparable insulin resistance in extrahepatic tissues on an HFD. Hepatic insulin resistance in response to high-fat feeding was more prominent in the HIP rats. We previously reported that the loss of β-cell mass in the HIP rat leads to hepatic insulin resistance (18). One possible explanation for this finding is that the impaired pulsatile delivery of insulin to the liver leads to hepatic insulin resistance. In health, insulin is secreted in discrete insulin secretory bursts that present the liver with an insulin concentration profile that oscillates with an amplitude of ~1,000 pmol/l in the fasting state and up to 5,000 pmol/l after meal ingestion (34,35), an observation recently confirmed in vivo in rats (26). The magnitude of these bursts is substantially decreased in patients with type 2 diabetes (36) and in animal models of reduced β-cell mass (37,38), including the HIP rat (A.V.P. and P.C.B., unpublished observations). It has been proposed that pulsatile mode of insulin delivery to liver increases hepatic insulin sensitivity (39,40), possibly by avoiding insulin receptor downregulation and/or sustained activation of AKT with attendant feedback inhibition of IRS-2 (41). We postulate that the more prominent hepatic insulin resistance in the HIP rat on an HFD (and in obese patients with type 2 diabetes) may relate at least in part to the decline in β-cell mass leading to an abnormal pattern of insulin delivery to the liver.

We also document a decrease in hepatic insulin clearance in HIP rats fed an HFD. Although fasting insulin levels in HIP rats increased almost threefold in response to an HFD, C-peptide levels remained relatively unchanged (Table 1). Thus, in the HIP rat, the C-peptide–to–insulin molar ratio, a measure of insulin clearance, was reduced by 40% in high fat–fed HIP rats. We have previously reported that the amplitude of insulin pulses directed to

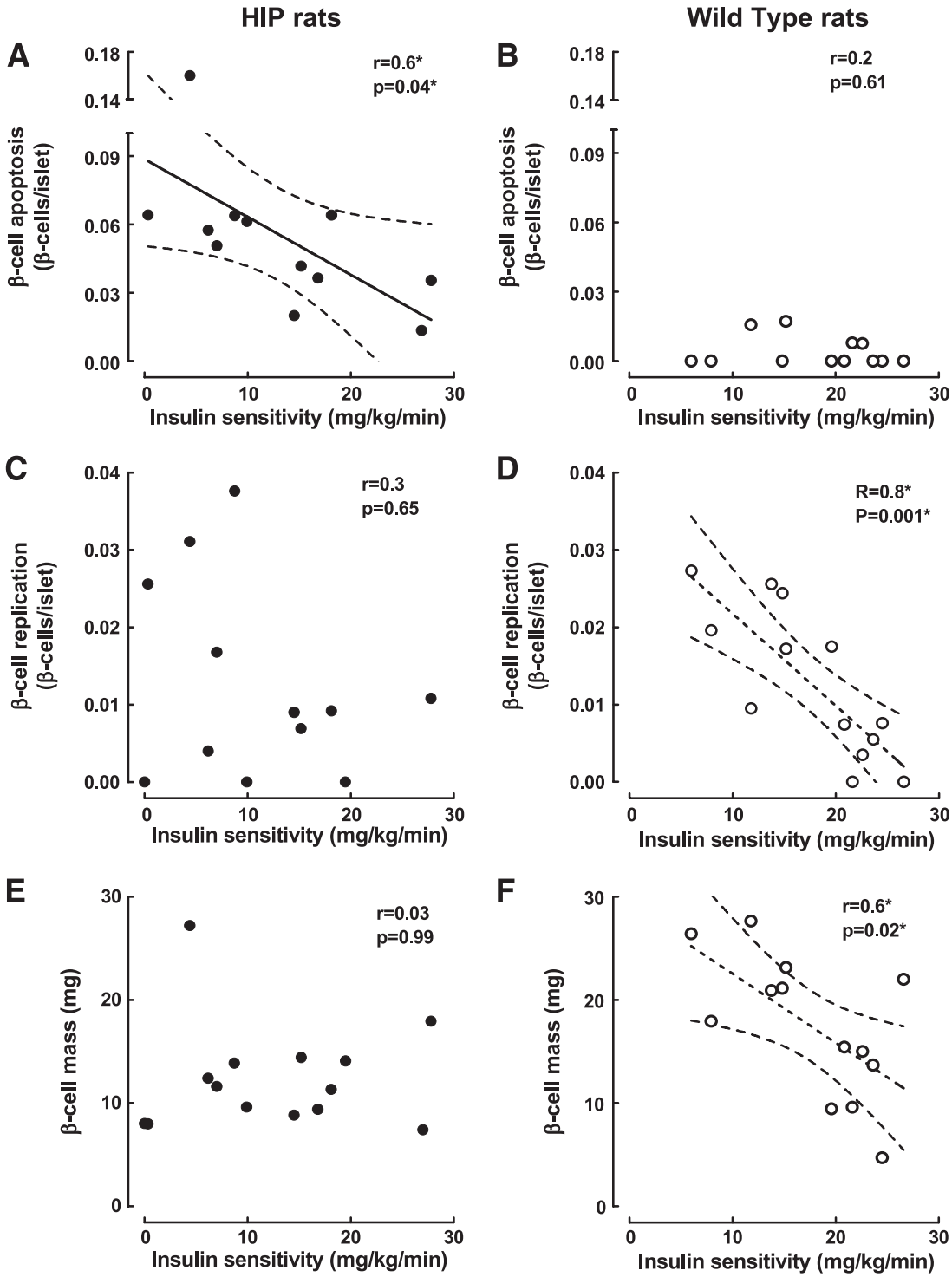

FIG. 7. HFD-induced insulin resistance correlates with the increase in β-cell apoptosis in HIP rats and increase in β-cell replication in WT rats. Regression analysis of relations among the β-cell apoptosis, β-cell replication, and β-cell mass versus hyperinsulinemic-euglycemic clamp determined insulin sensitivity in WT rats (n = 13) (*B*, *D*, and *F*) and HIP rats (n = 14) (*A*, *C*, and *E*) after 10-week treatment with 60% HFD or regular chow.

the liver is directly related to hepatic insulin clearance in humans (42). Consistent with this hypothesis, hepatic insulin clearance is decreased in animal models of reduced β-cell mass/insulin pulse mass as well as in humans with diabetes (37,38,43,44). Because hepatic insulin extraction depends on the amplitude of insulin pulses presented to the liver (42), deficits in insulin secretion, at least in the fasting state, would be largely offset in the systemic circulation by decreased hepatic insulin clearance.

In summary, an HFD induced a comparable increase in expression of IAPP and induction of UPR in β-cells irrespective of amyloidogenic potential of expressed IAPP. However, despite the induction of the UPR, an HFD still led to β-cell ER stress–mediated apoptosis in the HIP but not WT rats with islet pathology that recapitulates that in humans with type 2 diabetes. Specifically, the β-cell mass was deficient in the high fat–fed HIP rats, because the increased β-cell apoptosis prevented an appropriate adap-

tive increase in β-cell mass. The consequence of β-cell ER stress and a deficit in β-cell mass in high fat–fed HIP rats were impaired insulin secretion and hyperglycemia. This β-cell failure led to a further exacerbation of the HFD-induced insulin resistance in the HIP rat.

ACKNOWLEDGMENTS

Studies were supported by grants from the National Institutes of Health (NIH) (DK59579) and the Larry Hillblom Foundation to P.C.B. A.V.M. is supported by the NIH Ruth L. Kirschstein National Research Service Award.

No potential conflicts of interest relevant to this article were reported.

We thank Heather Cox and Ryan Galasso for their excellent technical support and acknowledge the support and excellent suggestions of our colleagues at the Larry Hillblom Islet Research Center, Dr. Anil Bhushan, Dr. Senta Georgia, and Dr. Walter Soeller at Pfizer.

REFERENCES

1. Carey DG, Jenkins AB, Campbell LV, Freund J, Chisholm DJ: Abdominal fat and insulin resistance in normal and overweight women: direct measurements reveal a strong relationship in subjects at both low and high risk of NIDDM. *Diabetes* 45:633–638, 1996
2. Yki-Jarvinen H: Role of insulin resistance in the pathogenesis of NIDDM. *Diabetologia* 38:1378–1388, 1995
3. DeFronzo RA, Bonadonna RC, Ferrannini E: Pathogenesis of NIDDM. A balanced overview. *Diabetes Care* 15:318–368, 1992
4. Chan JM, Rimm EB, Colditz GA, Stampfer MJ, Willett WC: Obesity, fat distribution, and weight gain as risk factors for clinical diabetes in men. *Diabetes Care* 17:961–969, 1994
5. Seltzer HS, Allen EW, Herron AL Jr, Brennan MT: Insulin secretion in response to glycemic stimulus: relation of delayed initial release to carbohydrate intolerance in mild diabetes. *J Clin Invest* 46:323–335, 1967
6. Polonsky KS, Given BD, Van Cauter E: Twenty-four-hour profiles and pulsatile patterns of insulin secretion in normal and obese subjects. *J Clin Invest* 81:442–448, 1988
7. Perley MJ, Kipnis DM: Plasma insulin responses to oral and intravenous glucose: studies in normal and diabetic subjects. *J Clin Invest* 46:1954–1962, 1967
8. Temple RC, Carrington CA, Luzio SD, Owens DR, Schneider AE, Sobey WJ, Hales CN: Insulin deficiency in non-insulin-dependent diabetes. *Lancet* 1:293–295, 1989
9. Zeggini E, Weedon MN, Lindgren CM, Frayling TM, Elliott KS, Lango H, Timpson NJ, Perry JR, Rayner NW, Freathy RM, Barrett JC, Shields B, Morris AP, Ellard S, Groves CJ, Harries LW, Marchini JL, Owen KR, Knight B, Cardon LR, Walker M, Hitman GA, Morris AD, Doney AS, McCarthy MI, Hattersley AT: Replication of genome-wide association signals in UK samples reveals risk loci for type 2 diabetes. *Science* 316:1336–1341, 2007
10. Grant SF, Thorleifsson G, Reynisdottir I, Benediktsson R, Manolescu A, Sainz J, Helgason A, Stefansson H, Emilsson V, Helgadottir A, Styrkarsdottir U, Magnusson KP, Walters GB, Palsdottir E, Jonsdottir T, Gudmundsdottir T, Gylfason A, Saemundsdottir J, Wilensky RL, Reilly MP, Rader DJ, Bagger Y, Christiansen C, Gudnason V, Sigurdsson G, Thorsteinsdottir U, Gulcher JR, Kong A, Stefansson K: Variant of transcription factor 7-like 2 (TCF7L2) gene confers risk of type 2 diabetes. *Nat Genet* 38:320–323, 2006
11. Steinthorsdottir V, Thorleifsson G, Reynisdottir I, Benediktsson R, Jonsdottir T, Walters GB, Styrkarsdottir U, Gretarsdottir S, Emilsson V, Ghosh S, Baker A, Snorradottir S, Bjarnason H, Ng MC, Hansen T, Bagger Y, Wilensky RL, Reilly MP, Adeyemo A, Chen Y, Zhou J, Gudnason V, Chen G, Huang H, Lashley K, Doumatey A, So WY, Ma RC, Andersen G, Borch-Johnsen K, Jorgensen T, van Vliet-Ostaptchouk JV, Hofker MH, Wijmenga C, Christiansen C, Rader DJ, Rotimi C, Gurney M, Chan JC, Pedersen O, Sigurdsson G, Gulcher JR, Thorsteinsdottir U, Kong A, Stefansson K: A variant in CDKAL1 influences insulin response and risk of type 2 diabetes. *Nat Genet* 39:770–775, 2007
12. Butler AE, Janson J, Bonner-Weir S, Ritzel R, Rizza RA, Butler PC: Beta-cell deficit and increased beta-cell apoptosis in humans with type 2 diabetes. *Diabetes* 52:102–110, 2003
13. Kloppel G, Lohr M, Habich K, Oberholzer M, Heitz PU: Islet pathology and the pathogenesis of type 1 and type 2 diabetes revisited. *Surv Synth Pathol Res* 4:110–125, 1985
14. Hoppener JW, Oosterwijk C, Nieuwenhuis MG, Posthuma G, Thijssen JH, Vroom TM, Ahren B, Lips CJ: Extensive islet amyloid formation is induced by development of type II diabetes and contributes to its progression: pathogenesis of diabetes in a mouse model. *Diabetologia* 42:427–434, 1999
15. Butler AE, Janson J, Soeller WC, Butler PC: Increased beta-cell apoptosis prevents adaptive increase in beta-cell mass in mouse model of type 2 diabetes: evidence for role of islet amyloid formation rather than direct action of amyloid. *Diabetes* 52:2304–2314, 2003
16. Butler AE, Jang J, Gurlo T, Carty MD, Soeller WC, Butler PC: Diabetes due to a progressive defect in beta-cell mass in rats transgenic for human islet amyloid polypeptide (HIP rat): a new model for type 2 diabetes. *Diabetes* 53:1509–1516, 2004
17. Janson J, Soeller WC, Roche PC, Nelson RT, Torchia AJ, Kreutter DK, Butler PC: Spontaneous diabetes in transgenic mice expressing human islet amyloid polypeptide. *Proc Natl Acad Sci U S A* 93:7283–7288, 1996
18. Matveyenko AV, Butler PC: Beta-cell deficit due to increased apoptosis in the human islet amyloid polypeptide transgenic (HIP) rat recapitulates the metabolic defects present in type 2 diabetes. *Diabetes* 55:2106–2114, 2006
19. Huang CJ, Haataja L, Gurlo T, Butler AE, Wu X, Soeller WC, Butler PC: Induction of endoplasmic reticulum stress-induced beta-cell apoptosis and accumulation of polyubiquitinated proteins by human islet amyloid polypeptide. *Am J Physiol Endocrinol Metab* 293:E1656–1662, 2007
20. Huang CJ, Lin CY, Haataja L, Gurlo T, Butler AE, Rizza RA, Butler PC: High expression rates of human islet amyloid polypeptide induce endoplasmic reticulum stress mediated beta-cell apoptosis, a characteristic of humans with type 2 but not type 1 diabetes. *Diabetes* 56:2016–2027, 2007
21. Hardy J, Selkoe DJ: The amyloid hypothesis of Alzheimer's disease: progress and problems on the road to therapeutics. *Science* 297:353–356, 2002
22. Lindholm D, Wootz H, Korhonen L: ER stress and neurodegenerative diseases. *Cell Death Differ* 13:385–392, 2006
23. Tanzi RE, Bertram L: Twenty years of the Alzheimer's disease amyloid hypothesis: a genetic perspective. *Cell* 120:545–555, 2005
24. Haataja L, Gurlo T, Huang CJ, Butler PC: Islet amyloid in type 2 diabetes, and the toxic oligomer hypothesis. *Endocr Rev* 29:303–316, 2008
25. Novials A, Sarri Y, Casamitjana R, Rivera F, Gomis R: Regulation of islet amyloid polypeptide in human pancreatic islets. *Diabetes* 42:1514–1519, 1993
26. Matveyenko AV, Veldhuis JD, Butler PC: Measurement of pulsatile insulin secretion in the rat: direct sampling from the hepatic portal vein. *Am J Physiol Endocrinol Metab* 295:E569–574, 2008
27. Kahn SE, Prigeon RL, McCulloch DK, Boyko EJ, Bergman RN, Schwartz MW, Neifing JL, Ward WK, Beard JC, Palmer JP, et al.: Quantification of the relationship between insulin sensitivity and beta-cell function in human subjects. Evidence for a hyperbolic function. *Diabetes* 42:1663–1672, 1993
28. Bergman RN, Phillips LS, Cobelli C: Physiologic evaluation of factors controlling glucose tolerance in man: measurement of insulin sensitivity and beta-cell glucose sensitivity from the response to intravenous glucose. *J Clin Invest* 68:1456–1467, 1981
29. Laybutt DR, Preston AM, Akerfeldt MC, Kench JG, Busch AK, Biankin AV, Biden TJ: Endoplasmic reticulum stress contributes to beta cell apoptosis in type 2 diabetes. *Diabetologia* 50:752–763, 2007
30. DeFronzo RA, Soman V, Sherwin RS, Hendler R, Felig P: Insulin binding to monocytes and insulin action in human obesity, starvation, and refeeding. *J Clin Invest* 62:204–213, 1978
31. Ritzel RA, Butler PC: Replication increases beta-cell vulnerability to human islet amyloid polypeptide-induced apoptosis. *Diabetes* 52:1701–1708, 2003
32. Kaufman RJ: Orchestrating the unfolded protein response in health and disease. *J Clin Invest* 110:1389–1398, 2002
33. Bertolotti A, Zhang Y, Hendershot LM, Harding HP, Ron D: Dynamic interaction of BiP and ER stress transducers in the unfolded-protein response. *Nat Cell Biol* 2:326–332, 2000
34. Porksen N, Munn S, Steers J, Vore S, Veldhuis J, Butler P: Pulsatile insulin secretion accounts for 70% of total insulin secretion during fasting. *Am J Physiol* 269:E478–488, 1995
35. Porksen N, Munn S, Steers J, Veldhuis JD, Butler PC: Effects of glucose ingestion versus infusion on pulsatile insulin secretion. The incretin effect is achieved by amplification of insulin secretory burst mass. *Diabetes* 45:1317–1323, 1996
36. Laedtke T, Kjems L, Porksen N, Schmitz O, Veldhuis J, Kao PC, Butler PC: Overnight inhibition of insulin secretion restores pulsatility and proinsulin/insulin ratio in type 2 diabetes. *Am J Physiol Endocrinol Metab* 279:E520–528, 2000
37. Kjems LL, Kirby BM, Welsh EM, Veldhuis JD, Straume M, McIntyre SS, Yang D, Lefebvre P, Butler PC: Decrease in beta-cell mass leads to impaired pulsatile insulin secretion, reduced postprandial hepatic insulin

clearance, and relative hyperglucagonemia in the minipig. *Diabetes* 50: 2001–2012, 2001
38. Matveyenko AV, Veldhuis JD, Butler PC: Mechanisms of impaired fasting glucose and glucose intolerance induced by ~50% pancreatectomy. *Diabetes* 55:2347–2356, 2006
39. Komjati M, Bratusch-Marrain P, Waldhausl W: Superior efficacy of pulsatile versus continuous hormone exposure on hepatic glucose production in vitro. *Endocrinology* 118:312–319, 1986
40. Bratusch-Marrain PR, Komjati M, Waldhausl WK: Efficacy of pulsatile versus continuous insulin administration on hepatic glucose production and glucose utilization in type I diabetic humans. *Diabetes* 35:922–926, 1986
41. Hirashima Y, Tsuruzoe K, Kodama S, Igata M, Toyonaga T, Ueki K, Kahn CR, Araki E: Insulin down-regulates insulin receptor substrate-2 expression through the phosphatidylinositol 3-kinase/Akt pathway. *J Endocrinol* 179:253–266, 2003
42. Meier JJ, Veldhuis JD, Butler PC: Pulsatile insulin secretion dictates systemic insulin delivery by regulating hepatic insulin extraction in humans. *Diabetes* 54:1649–1656, 2005
43. Bonora E, Zavaroni I, Coscelli C, Butturini U: Decreased hepatic insulin extraction in subjects with mild glucose intolerance. *Metabolism* 32:438–446, 1983
44. Sando H, Lee YS, Iwamoto Y, Ikeuchi M, Kosaka K: Isoproterenol-stimulated C-peptide and insulin secretion in diabetic and nonobese normal subjects: decreased hepatic extraction of endogenous insulin in diabetes. *J Clin Endocrinol Metab* 51:1143–1149, 1980